Prompt-fission observable and fission yield calculations for actinides by TALYS

Kazuki Fujio[1,*], *Ali* Al-Adili[2], *Fredrik* Nordström[2], *Jean-François* Lemaître[3], *Shin* Okumura[4], *Satoshi* Chiba[1,5], and *Arjan* Koning[4]

[1]Tokyo Institute of Technology, 2-12-1 Ookayama, Meguro, 152-8550, Tokyo, Japan
[2]Department of Physics and Astronomy, Uppsala University, S-751 20, Uppsala, Sweden
[3]CEA-DAM Île-de-France, Bruyères-le-Châtel, 91297, Arpajon Cedex, France
[4]NAPC-Nuclear Data Section, International Atomic Energy Agency, Vienna International Centre, 1400, Vienna, Austria
[5]NAT Research Center, NAT Corporation, 3129-45 Hibara, Muramatsu, Tokai-mura, Naka-gun, 319-1112, Ibaraki, Japan

Abstract.
The nuclear reaction code TALYS adopts the Hauser-Feshbach statistical decay theory, to de-excite fission fragments. This involves for instance the evaporation of prompt fission neutrons and γ-rays. TALYS incorporates databases of primary fission fragment distribution which consists of primary fission fragment yield and data for excitation energy distribution of fission fragments. We conducted a sensitivity study on three parameters in TALYS and fitted them in order to reproduce experimental and evaluated data, in thermal neutron-induced fission of ^{235}U. Moreover, we demonstrate a large-scale calculation of average prompt neutron and γ-ray multiplicities for 243 selected actinide isotopes.

1 Introduction

Accurate evaluation of fission characteristics following the emission of prompt neutrons, known as prompt fission observables, is crucial for both scientific understanding and engineering applications. This includes gaining insights into nucleosynthesis in the universe and designing safe and efficient nuclear reactors. Empirical models [1, 2], Monte-Carlo samplings [3–9], and deterministic approaches [10–13] have been developed for evaluating prompt fission observables. The nuclear reaction code TALYS [14] (version:1.96) has been adapted to perform Hauser-Feshbach statistical decay calculations for each fission fragment. TALYS employs a deterministic technique using databases of primary fission fragment distribution implemented to calculate the first-chance fission. The databases provide the pre-neutron emission physical quantities that are necessary for generating the initial excitation energy distribution of fission fragments for each incident energy and fissioning nuclide. Several computational codes have been employed as pre-neutron fission fragment generators to prepare these physical quantities, enabling TALYS to calculate prompt fission observables and facilitate comprehensive comparisons between the adopted fission data.

*e-mail: fujio.k.aa@m.titech.ac.jp

© The Authors, published by EDP Sciences. This is an open access article distributed under the terms of the Creative Commons Attribution License 4.0 (https://creativecommons.org/licenses/by/4.0/).

In this study, we investigate the sensitivity of the calculated fission observables on parameters related to the spin-parity distribution and on the number of continuum states. We employ databases from both the GEF [9] and HF^{3}D models [11, 12], to search for the optimal parameter values in comparison to experimental and evaluated data. We also demonstrate the wider applicability of our methodology by showing the neutron and γ-ray multiplicities for a wide range of actinide isotopes as target nuclei in neutron-induced fission reactions.

2 Fission fragment de-excitation in TALYS

2.1 Fission model in TALYS

TALYS implements the fission fragment database to perform Hauser-Feshbach calculations for fission fragments. The pre-neutron data is tabulated in the database and consists of the primary fission fragment yield $Y_{\rm ff}(Z, A)$ for each fragment charge Z and mass number A, the mean excitation energy $\bar{E}_x$ of its Gaussian distribution, its width σ_{E_x}, and the average total kinetic energy $\overline{\rm TKE}$ for fragment pair to generate initial excitation energy distribution. Here, the models implemented in TALYS for $(Y_{\rm ff}(Z, A), \bar{E}_x, \sigma_{E_x}, \overline{\rm TKE})$ data are introduced.

GEF is a Monte-Carlo-based phenomenological fission model, which can be used to feed TALYS with synthetic primary fission fragment mass- and energy yields. The data are obtained from GEF (version:2021/1.2), and Monte-Carlo sampling was performed with 1 million fission events for each nuclide and for each incident energy. TALYS contains the GEF-generated pre-neutron data for 737 nuclei ranging from $_{76}$Os to $_{115}$Mc at excitation energies ranging from 0 up to 20 MeV.

TALYS also has primary fission fragment data from HF^{3}D for the neutron-induced fission of ^{235}U, ^{238}U, and ^{239}Pu. These data were prepared in a fully deterministic approach with fitting functions that are determined to reproduce experimental results. The mass distribution $Y_{\rm ff}(A)$ and TKE distribution $\overline{\rm TKE}(A)$ of primary fragments are generated to reproduce the experimental $Y_{\rm ff}(A)$ and $\overline{\rm TKE}(A)$, and the charge distribution is obtained from Wahl's Z_p model [1]. R_T model is employed for partitioning the excitation energy of the compound nucleus into two primary fission fragments. More details can be found in Ref. [11].

The third database incorporated in TALYS originates from the SPY model. The primary fission fragment distribution of SPY is obtained from a statistical scission point model using microscopic calculation, and see Ref. [15] for details.

Moreover, users can calculate prompt fission observables using arbitrary fission fragment data by preparing the same table format as TALYS. For details, refer to Ref. [14, 16].

2.2 Initial distribution in TALYS

TALYS builds the initial population for Hauser-Feshbach statistical decay calculation with an excitation energy distribution $G(E_x)$ and a spin-parity distribution $R(J, \pi, E_x)$. The excitation energy distribution in TALYS is represented by a Gaussian distribution with the mean excitation energy $\bar{E}_x$ and its width σ_{E_x}:

$$G(E_x) = \frac{1}{\sqrt{2\pi}\sigma_{E_x}} \exp\left\{-\frac{(E_x - \bar{E}_x)^2}{2\sigma_{E_x}^2}\right\}. \tag{1}$$

The spin-parity distribution is expressed as follows:

$$R(J, \pi, E_x) = \frac{1}{2} \cdot \frac{2J+1}{2f^2\sigma^2(E_x)} \exp\left\{-\frac{(J+1/2)^2}{2f^2\sigma^2(E_x)}\right\}, \tag{2}$$

where f^2 is a scaling factor, which governs the distribution of angular momenta in primary fission fragments. This parameter only affects the primary fragments and assures a reasonable agreement with prompt fission observables of experimental data. The spin cut-off parameter $\sigma^2(E_x)$ is defined as $\sigma^2(E_x) = 0.01389A^{5/3}/\tilde{a}\sqrt{a(E_x - \Delta)}$, where Δ is the pairing energy correction, $\tilde{a}$ is the asymptotic level density parameter, and a is the level density parameter. TALYS has another scaling factor, f_s, which controls a global adjustment of the spin cut-off parameter. This impacts all secondary fission fragments and products, and is applicable to the level density model.

3 Results and Discussion

3.1 Sensitivity of prompt fission observables on TALYS parameters

In a recent investigation, we presented a detailed sensitivity study on the TALYS model parameters relevant for the fission fragment de-excitation methodology [17]. For instance, the scaling factors f^2 and f_s were found to have a major influence on the prompt fission observables, because they change the spin-parity distribution of the primary and secondary fragments and independent fission products. Moreover, we investigated the effect of the number of continuum states N because it changes not only the number of states that fission fragments can transition and affects the prompt fission observables but also the computational time. It is given by

$$N = (E_x^{\max} - E_x^{\text{level}})/\Delta_{\text{bins}}(Z, A), \tag{3}$$

where $\Delta_{\text{bins}}(Z, A)$ is the energy width of discretized continuum state, $E_x^{\max}$ is the maximum excitation energy, and E_x^{level} is the excitation energy of the last discrete level. The prompt fission observables were calculated using $(Y_{\text{ff}}(Z, A), \bar{E}_x, \sigma_{E_x}, \overline{\text{TKE}})$ from HF^{3}D model and identified the parameter values $f^2 = 4$, $f_s = 0.4$, and $N = 300$, as optimal values to reproduce the neutron multiplicity and better γ-ray observables at thermal energy.

3.2 Calculation results for neutron-induced fission of ^{235}U using optimal parameter values

We employed TALYS to calculate the prompt fission observables of neutron-induced fission of ^{235}U, using fission fragment data from the GEF and HF^{3}D models. Furthermore, we compared the TALYS results with experimental and evaluated data. The label TALYS(GEF) is used to denote the TALYS calculations based on the GEF primary fission fragment distributions, whereas TALYS(HF^{3}D) denotes TALYS results using the primary fission fragment distributions from the HF^{3}D model. The results from the stand-alone GEF code are also included in the figures for comparison. In this section, we focus on the calculated prompt fission neutron multiplicity and show that TALYS results are in fairly good agreement with known data. More results can be found in Ref. [17].

The well known saw-tooth shape of the mass-dependent neutron multiplicities, $\nu_n(A)$, at thermal energy is well reproduced by TALYS with both used databases in Fig. 1 (a). Despite the differences in the decay methods, TALYS and GEF codes give fairly similar neutron multiplicity results. The average neutron multiplicities at thermal energy are 2.41 in TALYS(HF^{3}D), 2.30 in TALYS(GEF), and 2.41 in evaluated data. TALYS(GEF) underestimates the evaluated data at thermal energy by about 0.1 while TALYS(HF^{3}D) successfully reproduces the evaluated data as the original HF^{3}D model.

Figure 1 (b) represents $\nu_n(A)$ at two different incident neutron energies, namely 0.5 and 5.55 MeV. Müller et al. reported an enhanced $\nu_n(A)$ only from the heavy fragments [18].

This implies that the additional excitation energy brought to the compound nucleus is mainly dissipated by the heavy fragments, which is adopted in GEF via the energy-sorting mechanism [19]. As a consequence, we observe that $\nu_n(A)$ of TALYS(GEF) enhances only in the heavy fragments as the incident energy increases, since the neutron emission is governed by GEF's excitation energies. On the other hand, the results from TALYS(HF^{3}D) do not show this trend because the HF^{3}D model is adjusted to other data at higher excitation energies [11, 12]. TALYS will consequently produce results that reflect the energy-sorting adopted in each used model.

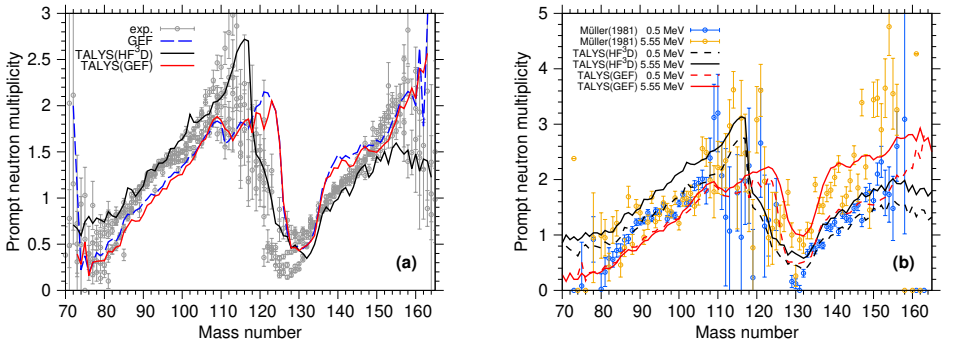

Figure 1. Calculated mass-dependent neutron multiplicities, $\nu_n(A)$, in the neutron-induced fission of ^{235}U (a) at thermal energy and (b) at the incident neutron energies of 0.5 and 5.55 MeV [18].

3.3 Global study on actinides

With the newly implemented feature to incorporate fission-fragment databases, TALYS now facilitates large-scale benchmarks to investigate systematic trends and biases in contemporary fission model codes. To demonstrate an example from such large-scale fission calculations, we performed a global fission comparison study based on the GEF databases [20]. Fission fragment distributions for 243 selected actinide isotopes were fed into TALYS. We employed the same parameters, namely $f^2 = 4$ and $f_s = 0.4$, as discussed in Sec. 3.1, while we adapted $N = 150$ to reduce computation time.

We showcase two calculated observables from the fission process, namely the average prompt fission neutron ($\bar{\nu}_n$) and γ-ray multiplicities ($\bar{\nu}_\gamma$). Systematic calculations of neutron emission by 1 MeV neutron-induced fission of actinides, from thorium to lawrencium, have been performed. The calculated neutron multiplicity is generally similar between TALYS(GEF) and stand-alone GEF (Fig. 2), albeit with a slight underestimation in TALYS(GEF). A zigzag pattern appears in both TALYS(GEF) and GEF results, which is due to the odd-even staggering of the neutron separation energy S_n of the compound nucleus since the excitation energy is provided by the capture of an incident neutron.

On the other hand, the calculated $\bar{\nu}_\gamma$ is plotted in Fig. 2, as a function of the neutron number of the compound nucleus, for 1 MeV incident neutron energy. We reported that $\bar{\nu}_\gamma$ decreases by approximately one by using $N = 150$ in neutron-induced fission reaction of ^{235}U in TALYS calculations [17]. It must be noted that ν_γ tends to be small with $N = 150$. In contrast to the prompt fission neutrons, the calculated $\bar{\nu}_\gamma$ reveals significant discrepancies at higher mass numbers and exhibits different global trends. Such systematic differences call for further scrutiny and comparison with experimental data.

The γ-ray data are known to be sensitive to the angular momentum population in the fragments. Thus, different treatments of the fragment angular momenta in GEF and TALYS could be one reason for such discrepancies. In order to properly evaluate the physical γ-ray trends and confirm the correct behavior, one needs to carefully analyze the correlation between the multiplicities and spectra of each observable, which is complicated especially in the absence of experimental data. Albeit beyond the scope of this work, in the future, we plan to investigate these discrepancies in view of the angular momentum generation in fission.

The key message from this global study is that fission models govern the fission yields and energies fed to TALYS, depending on the unique model assumptions. Therefore, the statistical decay in TALYS will be sensitive to the model descriptions and ingredients. By performing similar global comparative model studies, one can reveal systematic trends that shed light on model defects and systematic uncertainties in the model parameters.

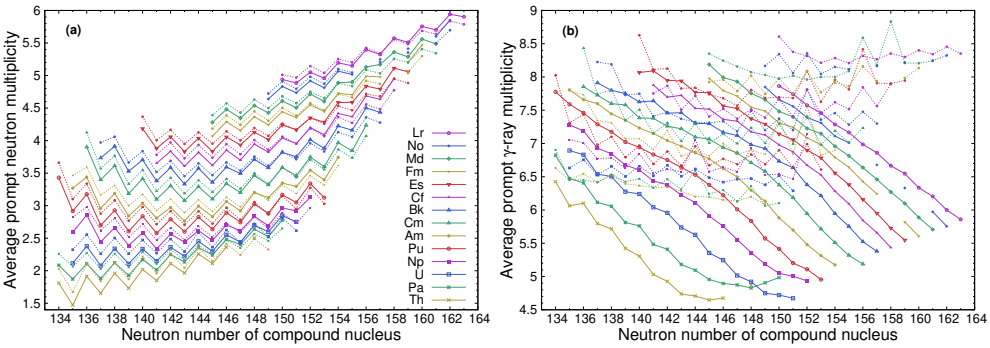

Figure 2. (a) Calculated average neutron multiplicities $\bar{\nu}_n$ and (b) calculated average γ-ray multiplicities $\bar{\nu}_\gamma$ as a function of the neutron number of the compound nucleus for 1 MeV incident neutron-induced fission of isotopes from Th to Lr. The solid lines correspond to the results of TALYS(GEF), while the dashed ones represent those of GEF.

4 Conclusion

TALYS was employed to calculate prompt fission observables by using the Hauser-Feshbach statistical decay theory. GEF, HF^{3}D, and SPY were used to generate databases of primary fission fragments in TALYS. The calculation using the database facilitates large-scale fission model benchmarks and verification, including the treatment of model defects and model parameter uncertainties.

We conducted a sensitivity study, to study the variations in the calculated prompt fission observables in TALYS, based on the parameters. We optimized the scaling factor for the primary fission fragment angular momentum population (f^2), the scaling factor for the spin cut-off parameter in the level density formula (f_s), and the number of continuum states (N), using the neutron-induced fission reaction of ^{235}U. We chose $f^2 = 4$, $f_s = 0.4$, and $N = 300$ as optimal values to accurately reproduce the neutron multiplicity and better γ-ray observables at thermal energy.

The calculated mass-dependent neutron multiplicities $\nu_n(A)$ showed an expected sawtooth shape and a decent agreement with experimental data at thermal energy. TALYS(GEF) exhibited an enhanced $\nu_n(A)$ at higher incident energies. But this was only observed in the heavy fragments, contrary to TALYS(HF^{3}D). The difference was attributed to the unequal energy-sorting mechanism in the models, which is reflected in the results of TALYS.

Finally, a large-scale global calculation was performed. TALYS(GEF) and GEF showed consistently similar trends in the average total neutron multiplicity, $\bar{\nu}_n$. However, the average total γ-ray multiplicity $\bar{\nu}_\gamma$ exhibited significant discrepancies, between the results of TALYS(GEF) and GEF. In this work, we focused on the neutron observables, and it was found that TALYS can reproduce the trends observed in prompt fission observables. In the future, we would like to account for the correlation with other fission observables such as isomeric ratios, γ-rays, and cumulative fission product yields.

Acknowledgements

The authors thank T. Kawano (Los Alamos National Laboratory) and K.-H. Schmidt for valuable discussions. The IAEA-NDS acknowledges the internship program "The Nuclear Regulation Human Resource Development Program (ANSET: Advanced Nuclear 3S Education and Training)" entrusted to Tokyo Institute of Technology, Tokyo, Japan by the Nuclear Regulation Agency of Japan, for supporting this work. A.A. would like to acknowledge Liljewalch travel scholarships and Ingegerd Berghs stiftelse for their research grants, in addition to Swedish Centre for Nuclear Technology (SKC). K. F. thanks C. Ishizuka and acknowledges her Grant-in-Aid for Scientific Research (B), MEXT, Japan, and by Japan Society for the Promotion of Science (JSPS) KAKENHI Grant Number 21H01856.

References

[1] A.C. Wahl, Atomic Data and Nuclear Data Tables **39**, 1 (1988)
[2] D.G. Madland, T.R. England, Nuclear Science and Engineering **64**, 859 (1977)
[3] P. Talou, B. Becker, T. Kawano, M.B. Chadwick, Y. Danon, Phys. Rev. C **83**, 064612 (2011)
[4] T. Kawano, P. Talou, M. Chadwick, T. Watanabe, J. Nucl. Sci. Technol. **47**, 462 (2010)
[5] J. Randrup, R. Vogt, Phys. Rev. C **80**, 024601 (2009)
[6] R. Vogt, J. Randrup, J. Pruet, W. Younes, Phys. Rev. C **80**, 044611 (2009)
[7] O. Litaize, O. Serot, Phys. Rev. C **82**, 054616 (2010)
[8] S. Lemaire, P. Talou, T. Kawano, M.B. Chadwick, D.G. Madland, Phys. Rev. C **72**, 024601 (2005)
[9] K.H. Schmidt, B. Jurado, C. Amouroux, C. Schmitt, Nuclear Data Sheets **131**, 107 (2016), special Issue on Nuclear Reaction Data
[10] A. Tudora, F.J. Hambsch, Eur. Phys. J. A **53**, 159 (2017)
[11] S. Okumura, T. Kawano, P. Jaffke, P. Talou, S. Chiba, J. Nucl. Sci. Technol. **55**, 1009 (2018)
[12] S. Okumura, T. Kawano, A.E. Lovell, T. Yoshida, J. Nucl. Sci. Technol. **59**, 96 (2022)
[13] A.E. Lovell, T. Kawano, S. Okumura, I. Stetcu, M.R. Mumpower, P. Talou, Phys. Rev. C **103**, 014615 (2021)
[14] A. Koning, S. Hilaire, S. Goriely, Eur. Phys. J. A **59**, 131 (2023)
[15] J.F. Lemaître, S. Goriely, S. Hilaire, J.L. Sida, Phys. Rev. C **99**, 034612 (2019)
[16] K. Fujio, S. Okumura, A. Koning, Tech. Rep. IAEA(NDS)-0239, International Atomic Energy Agency (2022)
[17] K. Fujio, A. Al-Adili, F. Nordström, J.F. Lemaître, S. Okumura, S. Chiba, A. Koning, Eur. Phys. J. A **59**, 178 (2023)
[18] R. Müller, A.A. Naqvi, F. Käppeler, F. Dickmann, Phys. Rev. C **29**, 885 (1984)
[19] K.H. Schmidt, B. Jurado, Phys. Rev. Lett. **104**, 212501 (2010)
[20] F. Nordström, Tech. Rep. UPTEC ES 21016, Uppsala university (2021)